

# We are IntechOpen, the world's leading publisher of Open Access books Built by scientists, for scientists

6,900

Open access books available

185,000

International authors and editors

200M

Downloads

Our authors are among the

154

Countries delivered to

TOP 1%

most cited scientists

12.2%

Contributors from top 500 universities



WEB OF SCIENCE™

Selection of our books indexed in the Book Citation Index  
in Web of Science™ Core Collection (BKCI)

Interested in publishing with us?  
Contact [book.department@intechopen.com](mailto:book.department@intechopen.com)

Numbers displayed above are based on latest data collected.  
For more information visit [www.intechopen.com](http://www.intechopen.com)



# Review of Rotary Switched Reluctance Machine Design and Parameters Effect Analysis

*Ana Camila Ferreira Mamede, José Roberto Camacho and Rui Esteves Araújo*

## Abstract

The switched reluctance machine (SRM) has gained much interest in industrial applications, wind power systems, and electric vehicles. This happened because its main disadvantages, such as the ripple in the torque, were overcome due to continuous research and its advantages, such as simple and robust construction, ability to operate at high speeds and variable speeds, insensitivity to high temperatures, and fault tolerance, have made the SRM the right machine for many applications. The SRM project is apparently similar to the traditional machine design, but diverges on several points due to the unique features of the SRM. Over the years, several authors have proposed different project methodologies for SRM, each with its own particularities and often contradicting each other. Thus, for a beginner designer, the SRM project is a challenge from choosing the right design methodology to choosing the values of some dimensions, which are often empirical. This chapter aims to offer the beginner designer a detailed review of the main SRM design methodologies. In addition, an effect analysis will provide useful insights on how each design variable affects machine performance. The designer will thus have important data on which to base his choices during the SRM design.

**Keywords:** switched reluctance machine, design, effect analysis, design of experiments, definitive screening design

## 1. Introduction

The switched reluctance machine (SRM) is a machine with double salience, that is, with stator and rotor poles, and this structure contributes to the production of a high output torque. Torque is produced by the alignment tendency of the poles; the rotor tends to move to a position where reluctance is minimized, and thus the inductance of the excited coil is maximized. Although the structure of the SRM is doubly salient, there is no winding or permanent magnets in the rotor [1], simplifying the structure of the machine and contributing to the low manufacturing cost.

SRMs differ from traditional electric machines both structurally and in their performance characteristics; however, there are some similarities. A crucial difference when comparing SRM to traditional machines is that the stator and rotor generally have different numbers of poles and cannot operate without an electronic

converter [2]. Other features of the SRM are simplicity of construction, absence of coils in the rotor, tolerance to phase failures, robustness, and low production cost.

The performance of the switched reluctance machine depends heavily on its design and control, which allows reduced ripple in torque and improved torque-speed characteristics [3]. Few researchers have addressed the problem of the sensitivity of SRM performance in relation to its dimensions. In [4] the authors investigated how to mitigate the torque ripple through the variation of SRM geometric parameters based on finite element simulation results. In [5] the effect of the variation of the dimensions was analyzed in relation to copper losses, gains in the machine weight, torque ripple, and average torque value. The analyses were based on the method proposed in [6].

As the design of SRM for a particular application is a compromise between various performance criteria, improvement of a performance parameter may result in the degradation of other important features [7]. Consequently, the designer has to look for solutions that are feasible for all performance parameters. In order to deal with this trade-off and achieve an efficient design, the application of multi-objective optimization techniques to the SRM design seems to be the most appropriate approach. Optimization techniques are known for analyzing a large volume of machines, which demands a high computational cost. However, if the influence of each parameter on the performance of the machine is known, the number of parameters in the optimization can be reduced, making the process faster and more efficient.

Design of experiments (DOE) is a mathematical methodology used for planning and conducting experiments as well as analyzing and interpreting data obtained from the experiments. It is a branch of applied statistics that is used for conducting scientific studies of a system, process, or product in which input variables are manipulated to investigate its effects on the measured response variable [8]. Over past two decades, DOE has been a very useful tool traditionally used for improvement of product quality and reliability [9]. The usage of DOE has been expanded across many industries as part of the decision-making process either in new product development, manufacturing processes, or improvement. It is not used only in engineering field but has also been used in administration, marketing, hospitals, pharmaceutical [10], food industry [11], energy and architecture [12], and chromatography [13]. DOE is applicable to physical processes as well as computer simulation models [14].

There are several DOE methods, such as one-factor-at-a-time, factorial design, central composite design, Latin hypercube design, and others. Each method has its particularities, such as quantity of factors, levels of factors, and number of experiments required, and this is what determines the choice of a method for a specific experiment. Some methods, such as one-factor-at-a-time, for example, will become impractical when more design variables are considered, because the number of experiments increases exponentially with the number of design variables [15]. The design of electric machines generally involves a large number of design variables, and since the relationship between variables is often nonlinear, a three-level experiment is more appropriate because it allows a better evaluation of the curvature in the factor-response relationship [15, 16]. Therefore, with the intention of reducing the computational cost, a three-level class known as definitive screening design (DSD) will be used, which is capable of capturing nonlinearity and identifying the main active effects with a low number of experiments [16].

The main objective of this chapter is to present an effective and direct methodology for SRM design and to indicate the impact of each variable on the machine's performance, showing how and how much each design parameter affects the SRM response.

## 2. Structure and operation of SRM

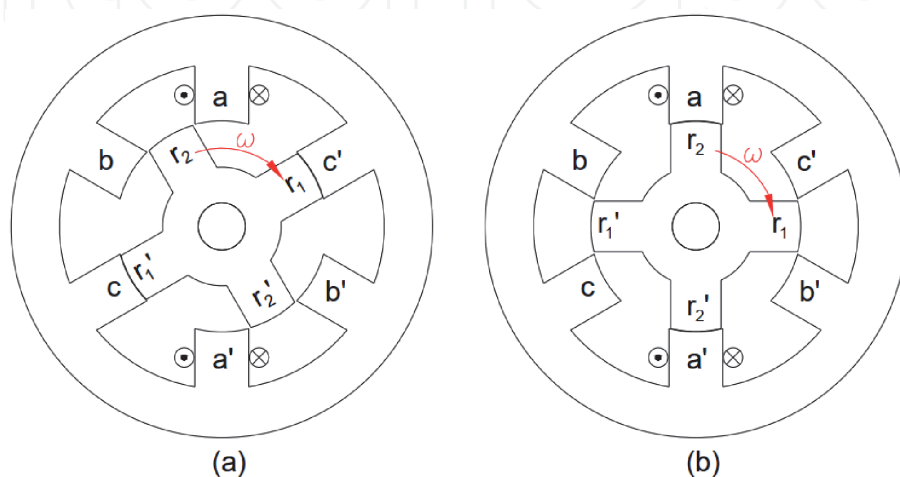
The operational principle of SRM is based on the power effects of the magnetic circuit that tend to minimize the reluctance of the magnetic circuit [2]. The rotor poles tend to align to the diametrically opposite poles of the stator whenever they are excited by a current [6]. If a pair of stator poles is excited, the rotor tries to turn to align with the poles of the stator so that the reluctance of the magnetic circuit would reach the minimum and also the energy of the magnetic circuit would thus be minimized [2]. When the energy minimum is reached, the magnetic forces try to keep the rotor in a position where the energy minimum of the magnetic circuit is preserved. Now, to make the machine rotate again, the magnetic energy must be removed to another pair of poles [2].

**Figure 1** shows a typical SRM with six stator poles and four rotor poles. Consider that the rotor poles  $r_1$  and  $r_1'$  and stator poles  $c$  and  $c'$  are aligned. By applying a current in phase  $a$ , a flux is established through the stator poles  $a$  and  $a'$  and  $r_2$  and  $r_2'$ , which tends to pull the rotor poles  $r_2$  and  $r_2'$  toward the stator poles  $a$  and  $a'$ . When they are aligned, the stator current of phase  $a$  is turned off, and phase  $b$  is excited [6].

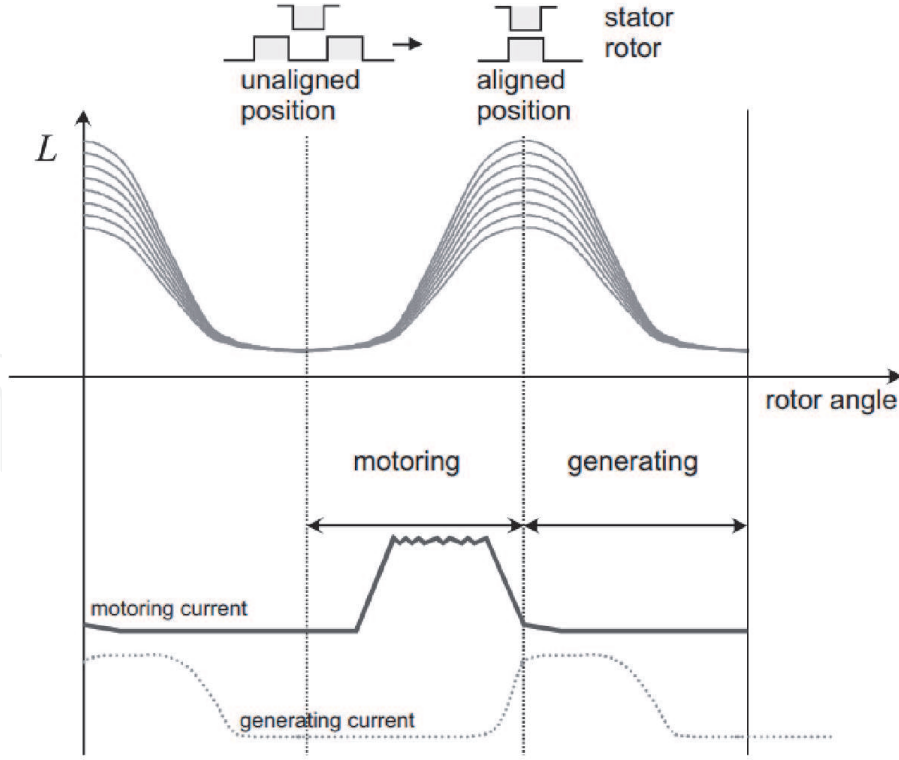
Due to the operating principle presented above, the self-inductance of each phase of the SRM changes according to the rotor position and current value, as shown in **Figure 2**. The same SRM can operate as both a motor and generator, depending on the moment of current injection. **Figure 2** shows the current pulses for each one.

If the magnetic flux of the SRM varies according to the position of the rotor and current, a group of curves  $\lambda(\theta, i)$ , known as magnetization curves, can be obtained and are fundamental for the study of this machine. The effect of saturation is evident in this figure and plays a key role in the SRM. The SRM is designed to achieve a certain level of saturation to maximize energy density, torque, and machine performance. The area delimited by the flux linkage in the aligned and unaligned position determines the mechanical output power of the machine; the greater the difference between these curves, or the inductance values in those positions, the higher the average torque value developed by the machine [2, 6].

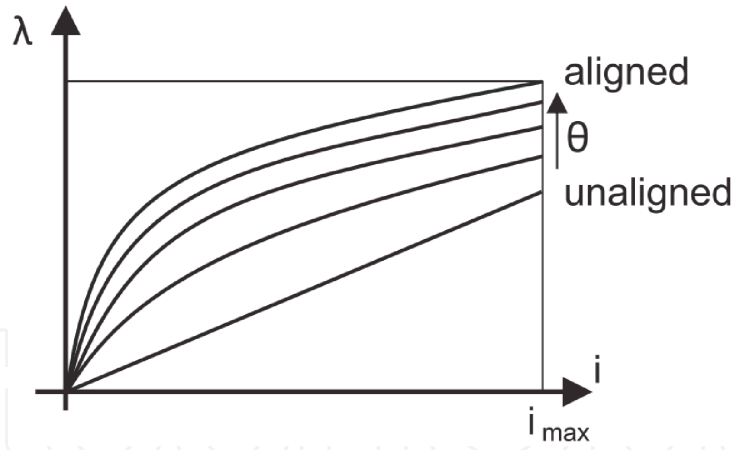
The calculation of the torque is a problem because of the dependence of the inductance of the magnetic circuit on both the rotor angle and the stator current. The dependence results from the excessive saturation of the magnetic circuit at certain rotor positions and with high stator currents (**Figure 3**) [2]. The torque developed is proportional to the area delimited by the curves in **Figure 3**, which



**Figure 1.**  
 Operation of an SRM. (a) Phase  $c$  aligned. (b) Phase  $a$  aligned. (Adapted from [6]).


**Figure 2.**

Inductance of a saturating reluctance motor as a function of rotor angle with current as a parameter, and the current pulses of a motor drive and a generator drive, when the voltage of the intermediate circuit remains constant [2].


**Figure 3.**

Magnetization curves.

corresponds to the stored magnetic energy, and can be calculated in terms of co-energy, current, and rotor position by

$$T_e = \left. \frac{\delta W'_f(i, \theta)}{\delta \theta} \right|_{i=\text{constant}} \quad (1)$$

with the co-energy  $W'_f$  being defined by

$$W'_f = \int \lambda(\theta, i) di. \quad (2)$$



The average torque can be calculated by assuming that the current  $I_p$  is maintained constant between the aligned and unaligned positions of the rotor and that the magnetization curve is available [6]. The area between the curve in the aligned position and the unaligned position is denoted as  $\delta W_m$  and corresponds to the work done by the machine cycle, which can be calculated from the co-energies, as shown in Eq. (3):

$$\delta W_m = \delta W'_{f-\text{aligned}} - \delta W'_{f-\text{unaligned}} \quad (3)$$

The trapezoidal integration, as long as a reasonable number of points are considered in the curve, offers good results. The average torque can be obtained through the total work performed by a machine revolution by Eq. (4), where  $N_s$  and  $N_r$  are the stator and rotor number of poles, respectively:

$$T_{ave} = \frac{\delta W_m N_s N_r}{2\pi} N \cdot m \quad (4)$$

### 3. Design procedures

The general theory that governs the design of an electric machine includes studies in the areas of electromagnetism, winding arrangements, magnetic circuit behavior, inductance, and winding resistance [2]. The process of designing an electric machine takes into account all these studies and the empirical knowledge acquired over the years by designers and researchers.

The design of a rotating electrical machine starts by defining certain basic characteristics, such as the type of machine, type of construction, rated power, rated rotational speed, number of pole pairs, operating frequency, rated voltage and number of phases, intended duty cycle, enclosure class, and structure of the machine [2]. In machine design there are a considerable number of free parameters. The task of finding an ideal solution becomes extremely complex unless the number of these parameters is somehow limited [2].

The difficulties of the SRM design can be attributed to several factors, including the following: (1) high magnetic and control nonlinearities; (2) many flexible design parameters, including those that affect vibrations and acoustic noises; (3) interdependence on the design of the converter and control parameters; (4) variable-speed operations; (5) thermal management due to the concentrated coils; (6) difficulty of thermal rating prediction; and (7) possible high sensitivity of design to manufacturing tolerance [17]. Also, during sizing process it is important to establish proper flux density values in the magnetic core. Very low values have the outcome of an unsaturated machine and low energy density, whereas very high values will limit the power developed and cause the core to heat up [18].

Too low values have the outcome of an unsaturated machine, and due to this, poor power density and too high values will limit the developed power and cause core heating [18].

Over the years, research has been based mainly on the design methodologies proposed by [6, 19], proposing changes and optimizing the project according to their acquired knowledge and application requirements [20–23]. The main difference between these two methods is the output equation used for the SRM. In [19], the author proposes a simplified output equation, and the choice of some coefficients is made through a table of typical values based on the application. A more complex output equation is presented by [6]; however, some of its parameters are

still chosen through ranges of typical values, which complicate the first steps in machine design.

The following design procedures are mainly based on [6, 24], presenting useful simplifications for manufacturing and some disagreements with other design methods. The process presented in this section corresponds to a simple and intuitive preliminary design of SRM for beginner designers. The calculation of the flux linkage at various machine positions will be done using the finite element method, performed in FEMM software.

### 3.1 Starting values

To design a machine for a specific application, one must know its characteristics, which will make up the SRM specifications. The design specifications for the SRM are the required output power  $P_{out}$  in W, the nominal speed  $n$  in rpm, the allowed peak current in A, and the available supply voltage for the system. From this data the mechanical torque of the machine is fixed and calculated through Eq. (5):

$$T_{mec} = \frac{P_{out}}{2\pi \frac{n}{60}} \quad (5)$$

**Figure 4** shows all the dimensions that must be determined for the construction of an SRM, where  $\beta_s$  is the stator polar arc,  $\beta_r$  is the rotor polar arc,  $w_{sp}$  is the width of the stator pole,  $b_{sy}$  is the stator back iron thickness,  $b_{ry}$  is the rotor back iron thickness,  $h_s$  is the height of the stator pole,  $h_r$  is the height of the rotor pole,  $D_{sh}$  is the diameter of the shaft,  $D_i$  is the inner diameter,  $D_o$  is the outer diameter, and  $g$  is the length of the air gap.

### 3.2 Inner, outer, and shaft diameter and core length

In general, the starting point for designing a machine is to obtain the SRM power output equation; this process is presented by [6], and from the output equation, other dimensions are determined. However, the output equation presented by [6]

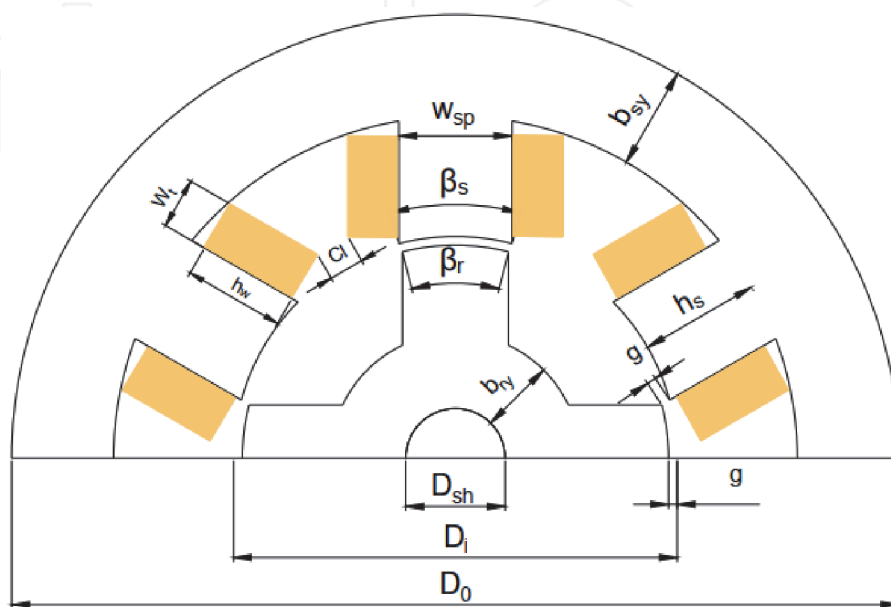


**Figure 4.**  
SRM dimensions.

presents a series of parameters that must be determined arbitrarily so that the calculation of the inner diameter is possible (such as length, efficiency, duty cycle, and specific electric charge, among others), which makes the process a little bit ambiguous. This process can be simplified by using tables presented by international standards such as [25], which determine typical frame values for all rotating machines.

Thus, the initial values for the frame, inner diameter, external diameter, shaft diameter, and core length are selected from tables that relate the output power, nominal velocity, and frame size ( $FS$ ) present in [25]. These values can be adjusted at the end of the sizing process. The outside diameter is calculated by

$$D_0 = (FS - x)2 \quad (6)$$

where  $x$  corresponds to the value of the foot of the machine, usually adopted as 3 mm. Normally, the internal diameter is 0.4–0.7 times the value of the external diameter [19].

The inner diameter is initially set equal to  $FS$ , but can be changed according to the need of the application and constructive limitations. In [6], the length of the core is determined as a multiple of the inner diameter ( $k_L$ ). The value of  $k_L$  is decided by the nature of the motor application and space limitation. For non-servo applications, the interval for  $k_L$  is given by Eq. (8) and for servo applications by Eq. (9):

$$L = k_L D_i \quad (7)$$

$$(0.25 \leq k_L \leq 0.7) \quad (8)$$

$$(1.0 \leq k_L \leq 3.0) \quad (9)$$

Therefore, since the frame has already been chosen, the upper limit of the core length is already defined, and the lower limit can be determined by the above equations.

### 3.3 Air gap length

For switched reluctance machines, the air gap length determines the output torque and the volt-ampere requirement in the motor drive. However, the air gap cannot be made as small as possible due to manufacturing constraints, and it is roughly proportional to the motor size [23]. In [6] the air gap value should be chosen according to the size of the machine; for small machines, with power less than 1.0 hp, the air gap should vary between 0.18 and 0.25 mm. Integral horsepower machines, with power above 1.0 hp, may have air gaps from 0.3 to 0.5 mm [6]. For other authors, the air gap length should be selected to be about 0.5–1% of the rotor diameter [2, 19].

### 3.4 Selection of number of phases and number of poles

The number of phases of an SRM is usually determined through factors, such as directional capacity, reliability, cost, and high speed operation, as described below.

1. Starting capability: In a single-phase SRM, for example, the cost with the control is low; however, there are regions where the torque produced is null, and the consequence of this is the impossibility of the machine being activated in these positions if no artifice is used, such as a permanent magnet.



2. Directional capability: In some applications it is necessary to change the direction of operation of the SRM, and this determines the minimum number of phases for that application. For example, a 4/6 machine is capable of providing unidirectional rotation only, whereas a 6/4 is capable of two-direction rotation. The former case is a two-phase machine, and the latter case is a three-phase SRM [6].
3. Cost: The cost of an SRM relates the cost of the motor itself and the cost of its converter, so a high number of phases demand a high number of power devices in the converter, increasing the total cost of the application and restricting its use to some applications.
4. Reliability: A higher number of phases mean a higher reliability because a failure of one or more phases will not prevent the machine from continuing to operate. This factor may be highly relevant in critical applications where safety of human beings or successful mission completion is the predominant factor [6].
5. Power density: A higher number of phases tend to provide a higher power density in the machine.
6. Efficient high-speed operation: Efficiency is enhanced by reducing the core loss at high speed by decreasing the number of stator phases and lowering the number of phase switchings per revolution [6]. In high-speed operations it is necessary to keep the motor size smaller, which requires a great reduction in losses to maintain the thermal robustness [6].

The limiting factors in the number of poles selection are the number of converter power switches and their associated cost of gate drives and logic power supplies and the control requirement in terms of small rise and fall times of the phase currents [6]. The topologies 6/4 and 8/6, three and four phases, respectively, are common in industry because they are cost-effective; however, other topologies are possible. An increase in the pole number improves the operational accuracy of the motor and the quality of the torque, but simultaneously the structure and control of the converter switches get more complicated [2]. Many applications such as fans or pumps and even in off- and on-highway vehicle propulsion can stand higher commutation torque ripples, for example, than position servos.

The stator frequency for a phase is determined by the maximum machine speed and number of rotor poles. By increasing the number of rotor poles, the frequency in the stator increases in proportion, resulting in higher core losses and greater conduction time to provide the rise and fall of the current than that of an SRM drive with a smaller number of rotor poles [6]. Therefore, the selection of number of phases and number of poles is directly related to the application requirements and available budget.

### **3.5 Stator and rotor pole arc**

The values of the stator pole arc and rotor pole arc are chosen to guarantee the proper starting of the machine and to shape the motor torque profile [6]. These requirements are inserted into the SRM project by offering a lower and upper limit for the values of the polar arcs. These restrictions are detailed in [1, 6, 19] and briefly described here.

In order to guarantee proper starting of the machine and to prevent the occurrence of parasitic currents due to the magnetic flux dispersion effect, the rotor polar arc must be larger than the polar arc of the stator [1, 6]:

$$\beta_r \geq \beta_s \tag{10}$$

Krishnan showed in [6] that the minimum value for polar arcs is set according to the number of poles of the machine by Eq. (11):

$$\min(\beta_s, \beta_r) = \frac{4\pi}{N_s N_r} \tag{11}$$

The angle between the corners of the adjacent rotor poles must be greater than the polar arc of the stator or there will be an overlap of the stator and rotor poles in the non-aligned position [24]. This implies that the minimum inductance value will be greater, reducing the difference between the maximum and minimum values, which leads to a reduction in the torque value. This relation is presented in Eq. (12):

$$\frac{2\pi}{N_r} - \beta_r > \beta_s \tag{12}$$

The conditions presented in Eqs. (10)–(12) can be represented graphically in a triangle of possibilities. It is necessary for the values of the polar arcs of the machine to be within this triangle [24]. **Figure 5** shows the triangle of possibilities for an SRM 6/4 and an SRM 8/6. For example, for an SRM 8/6, if  $\beta_s = 20^\circ$ , then  $20^\circ \leq \beta_r \leq 40^\circ$ . The feasible region restricts the possible combinations of stator and rotor pole angles but does not provide the best solution [26].

An optimum value can be solved for the pole size. This optimum value yields the maximum inductance ratio and simultaneously the maximum average torque. In addition, several other factors affecting the operation of the machine have to be taken into account, such as the torque ripple, starting torque, and the effects of saturation, and therefore no general solution can be attained [2]. Some authors have dedicated themselves to optimizing the values of the polar arcs [27–29].

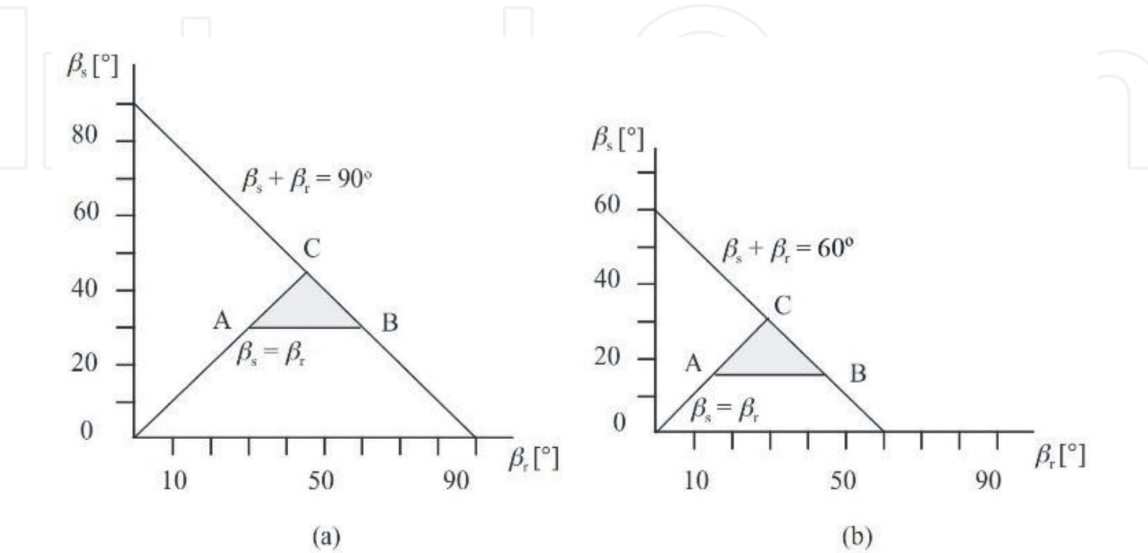


**Figure 5.** Triangle of possibilities for  $\beta_s$  and  $\beta_r$  of (a) a three-phase 6/4 SRM and (b) a four-phase 8/6 SRM (Adapted from [19]).

### 3.6 Preliminary design

With the previously defined dimensions, the other dimensions of **Figure 1** can be calculated as shown below. To begin, it is necessary to have access to the B-H characteristics of the material used for the stator and rotor blades; an example is shown in **Figure 6**. From the curve the “knee” point is determined and used to limit the flux density inside the motor. SRM is designed to achieve saturation; a saturated machine has the potential to convert approximately twice as much energy as the unsaturated machine to the same dimensions and peak current [30]. Thus, the value of flux density is defined in order to maximize the energy density and machine performance. Assuming the flux density at the stator pole  $B_s$  is equal to  $B_{max}$ , the remainder of the machine can be projected by estimating the value of the flux density at the other points.

The stator pole width is determined by the stator polar arc and by the value of inner diameter as follows:

$$w_{sp} = D_i \sin\left(\frac{\beta_s}{2}\right) \quad (13)$$

The stator back iron thickness has to be large enough to support half of the flux density passing through the stator pole. Therefore, the back iron thickness of the stator must be at least half the stator pole width. Due to considerations of mechanical robustness and minimization of vibration, it could have a value in the range of

$$w_{sp} > b_{sy} \geq 0.5w_{sp} \quad (14)$$

Next, the stator pole height can be calculated as

$$h_s = \frac{D_0 - 2b_{sy} - D_i}{2} \quad (15)$$

The rotor back iron thickness does not need be as much as the stator back iron thickness and neither has to be equal to the minimum value, which is equal to the minimum value of the stator back iron thickness. The rotor back iron thickness in terms of the stator pole width can be set in the range given below:

$$0.5w_{sp} < b_{ry} < 0.75w_{sp} \quad (16)$$

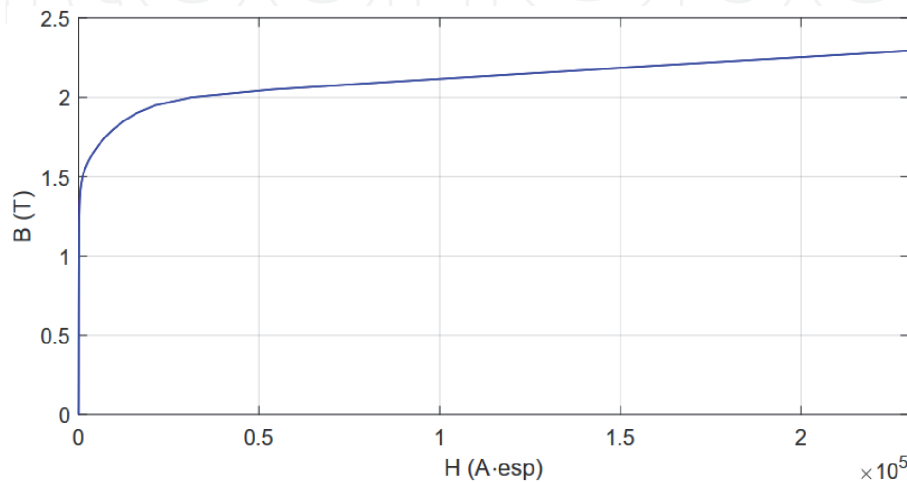


**Figure 6.**  
B-H curve for M19 steel.

According to Vijayraghavan [24], securing the flux density at the stator back iron thickness  $B_y$  as approximately half of the  $B_{max}$  value and the flux density in the  $B_{rc}$  as approximately 80% of the maximum value is a good practice for SRM projects, because it reduces acoustic noise in the machine. This means choosing the value of  $b_{sy}$  equal to the value of  $w_{sp}$ , upper limit of Eq. (14), and  $b_{ry}$  equal to  $0.625w_{sp}$ . These values can be adopted in a preliminary design, but can be optimized due to their influence on the volume and cost of the machine.

The height of the rotor pole can be determined as follows:

$$h_r = \frac{D_i - 2g - D_{sh} - 2b_{ry}}{2} \quad (17)$$

With these dimensions, the next step is the design of the coils, and for this it is necessary to analyze the magnetic circuit of the SRM, shown in **Figure 7**. The reluctances of the stator pole, yoke, rotor pole, rotor core, and air gap are represented by  $\mathfrak{R}_s$ ,  $\mathfrak{R}_y$ ,  $\mathfrak{R}_r$ ,  $\mathfrak{R}_{rc}$ , and  $\mathfrak{R}_g$ , respectively.

The equivalent reluctance of the equivalent magnetic circuit  $\mathfrak{R}_{eq}$  in **Figure 7** is obtained as

$$\mathfrak{R}_{eq} = 2(\mathfrak{R}_s + \mathfrak{R}_r + \mathfrak{R}_g) + \frac{\mathfrak{R}_{rc} + \mathfrak{R}_y}{2} \quad (18)$$

The reluctance  $\mathfrak{R}$  in a particular section can be calculated by Eq. (19), where  $H$  is the magnetic field intensity,  $l$  is the mean path length in the section,  $B$  is the flux density in the section,  $A$  is the area of the section, and  $\varphi$  is the flux in the section:

$$\mathfrak{R} = \frac{H l}{B A} = \frac{H l}{\varphi} \quad (19)$$

The magnetic circuit equation of aligned inductance can be written as

$$\mathcal{I}_{align} = NT i = \mathfrak{R}_{eq} \varphi \quad (20)$$

where  $NT$  is the number of turns per phase. The equations for calculating the length of sections, cross-sectional area, and respective value of  $B$  are shown in **Table 1**. Note that some values of flux density used follow the indications of [6, 24]. The value of  $H$  for each section is obtained through the B-H curve of the magnetic material when estimating the value of  $B$  for each section. We suggest the use of an interpolation algorithm.

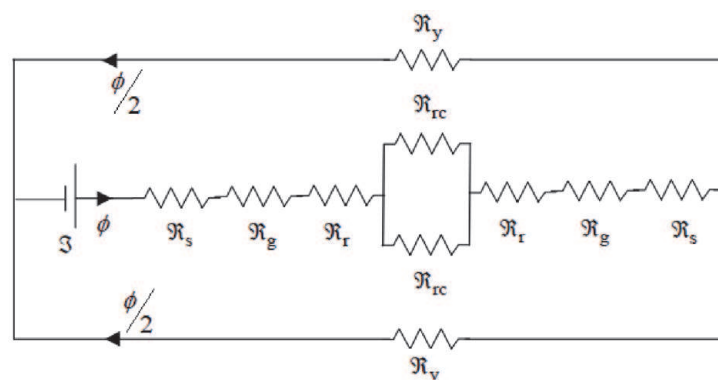


**Figure 7.**  
Magnetic circuit of the SRM.

Part	Length	Cross section	Flux density
Stator pole	$l_s = h_s + \frac{b_{sy}}{2}$	$A_s = \frac{D_i}{2} L \beta_s$	$B_s = B_{max}$
Stator back iron	$l_y = \pi \frac{(D_0 - b_{sy})}{2}$	$A_y = b_{sy} L$	$B_y = \frac{B_s}{2}$
Rotor pole	$l_r = \frac{(D_i - D_{sh})}{4} + \frac{(h_r - g)}{2}$	$A_r = \left(\frac{D_i}{2} - g\right) L \beta_r$	$B_r = \frac{B_s n A_s}{A_r}$
Rotor back iron	$l_{rc} = \pi \left( \frac{(D_i + D_{sh})}{4} - \frac{(h_r + g)}{2} \right)$	$A_{rc} = \left( \frac{(D_i - D_{sh})}{2} - h_r - g \right) L$	$B_{rc} = 0.8 B_s$
Air gap	$l_g = g$	$A_g = \frac{A_s + A_r}{2}$	$B_g = \frac{B_s A_s}{A_g}$

**Table 1.**  
Magnetic path lengths, cross sections, and flux densities.

Now, the total ampere-turns  $\mathfrak{I}$  required for the machine operation at full load can be calculated. The magnetic circuit equation is written as

$$\mathfrak{I} = NTi = 2(H_s l_s + H_r l_r + H_g l_g) + \frac{H_{rc} l_{rc}}{2} + \frac{H_y l_y}{2} \quad (21)$$

As the value of the peak current allowed in the machine was determined at the beginning of the design, the number of turns  $NT$  can be calculated through Eq. (21). The number of turns must be an integer and even. The value of the corrected current is then corrected through Eq. (22):

$$i_p^* = \frac{\mathfrak{I}}{NT} \quad (22)$$

The conductor area  $a_c$  can be calculated from the number of phases  $q$ , peak current value  $i_p$ , and current density  $J$ . The maximum permissible value of  $J$  is determined by the type of machine and cooling method employed [2, 6]. Usually, the value adopted for SRM during the preliminary project is  $J = 6 \text{ A/mm}^2$ :

$$a_c = \frac{i_p^*}{J \sqrt{q}} \quad (23)$$

The section of the normalized conductors is obtained by selecting the section closer but greater than the value obtained from Eq. (23). The wire diameter  $d_w$  including insulation is given by Eq. (24):

$$d_w = \sqrt{\frac{4a_c}{\pi}} + 0.1 \text{mm} \quad (24)$$

The coil must be placed between two consecutive stator poles, and to ensure that the winding fits, it is necessary to perform the following calculations. If necessary, the stator dimensions or conductor size can be changed. Assuming a wedge of  $h_{wedge}$  is required to hold the windings in place; the stator pole arc length  $t_s$  at the closest point of the winding to the center of the shaft is given by Eq. (25):

$$t_s = \left( \frac{D_i}{2} + h_{wedge} \right) \beta_s \quad (25)$$

Accounting for the wedges that hold the windings in place leads to the calculation of a modified stator pole pitch  $\lambda_s$  as in Eq. (26):



$$\lambda_s = \frac{\pi(D_i + 2h_{wedge})}{N_s} \quad (26)$$

The maximum height of the winding  $h_w$  which can be accommodated inclusive of the space required to place wedges that hold the windings in place is given by

$$h_w = h_s - h_{wedge}. \quad (27)$$

The number of layers that can be accommodated in this available winding height is given by Eq. (28), where  $f_f$  represents the field factor and is approximately equal to 0.95. The value of  $N_v$  is rounded off to the nearest lower integer:

$$N_v = \frac{h_w f_f}{d_w} \quad (28)$$

Now the number of horizontal layers required for winding is given by Eq. (29), and this value is rounded off to the nearest higher integer:

$$N_h = \frac{NT}{2N_v} + 1 \quad (29)$$

The width of the winding  $W_t$  is given by Eq. (30):

$$W_t = \frac{d_w N_h}{f_f} \quad (30)$$

The space between two stator pole tips at the bore is given by

$$Z = \lambda_s - t_s. \quad (31)$$

The clearance between the windings at the bore is given by

$$Cl = Z - 2W_t. \quad (32)$$

This value has to be positive and preferably greater than 3 mm. Naturally, the actual clearance between the windings will be slightly higher than the clearance calculated at the bore. If the clearance value is acceptable, the designer can proceed with the analysis, or else a different size conductor can be chosen, and the clearance can be checked again.

### 3.7 Design verification

The next step is to estimate the average torque value and check whether it matches the initial specifications, if the value obtained is not acceptable, it is necessary to modify the design. The average torque can be calculated from the values of the co-energies, according to Eq. (4), for which it is necessary to know the value of the flux linkage in the aligned and unaligned position for the peak current. These values can be determined analytically through different methods such as those presented by [6, 31] or can be obtained through a finite element simulation. Since there are several free and fast finite element simulation software packages available, we strongly suggest using them for the calculation of SRM characteristics.

The analysis of other characteristics of the SRM, such as calculation of losses in the copper and in the iron, by parasitic currents and hysteresis, is detailed by

[6, 24, 32–34]; however, they can also be obtained through finite element simulation. Thus, enough data are available to estimate the efficiency and other parameters of SRM. The control can be designed and the rest of the SRM characteristics determined.

### 3.8 Calculation of losses

The losses in the SRM are composed of copper losses and iron losses. The copper losses only appear in the stator, since there are no windings in the rotor, and can be calculated by

$$P_{cu} = qI^2R_s, \quad (33)$$

where  $R_s$  is the per-phase resistance of the stator winding and  $I$  is the rms value of the current given by

$$I = \frac{i_p}{\sqrt{q}} \quad (34)$$

Hence, the copper losses are

$$P_{cu} = i_p^2 R_s. \quad (35)$$

The resistance of a single phase can be computed in terms of the specific resistivity  $\rho$ , mean length of the winding  $l_m$ , and area of cross section of the conductor  $a_c$  by Eq. (36):

$$R_s = \frac{\rho l_m}{a_c} NT \quad (36)$$

The mean length of a winding turn is given by Eq. (37):

$$l_m = 2L + 4W_t + 2D_i \sin\left(\frac{\beta_s}{2}\right) \quad (37)$$

The iron losses can be split into two major portions, hysteresis and eddy current losses. Core losses are difficult to predict in the SRM due to the presence of flux densities with various frequencies in stator segments. Further, these flux densities are neither pure sinusoids nor constants [1, 33]. There are two papers that lead the calculation of core losses, the one developed in [33] and the one developed in [34].

The method proposed in [33] is simpler and provides a good estimate of the losses in the core, but does not clearly separate the hysteresis and eddy current losses. Manufacturers of lamination core steel provide data showing the variation of core loss (in watts per pound or kilogram) as a function of flux density and frequency [33]. Once the flux density and iron weight for each part of the machine are known, these data are used to calculate the losses in the core.

## 4. Dimensional effect analysis

The previous section presented the procedures for the preliminary design of the SRM, and it can be seen that many dimensions can be chosen within a range which, to a certain extent, influences the rest of the design and machine performance. Therefore, this section examines how and how much each dimension influences

Design variable	Type	Unit	Reference value	Range
$D_i$	Variable	mm	100	90–110
$D_o$	Variable	mm	190	185–195
$L$	Variable	mm	180	150–200
$g$	Variable	mm	0.4	0.3–0.5
$\beta_s$	Variable	deg	22.5	15–25
$\beta_r$	Variable	deg	22.5	15–30
$b_{sy}$	Variable	mm	19.509	9.7545–19.509
$b_{ry}$	Variable	mm	12.193	9.7545–14.632
$B_{max}$	Fixed	T	1.7	—
$D_{sh}$	Fixed	mm	28	—
Turns per phase	Fixed	units	152	—
Conductor area of cross section	17 AWG	—	—	—
Peak current	Fixed	A	12	—
Lamination material	M19	—	—	—

**Table 2.**  
*Details of 8/6 SRM analyzed.*

SRM performance through a new DOE class, a small three-level design that is presented by [16]. This study is an important and useful tool for machine designers, since it allows a basis for decisions for the optimization of the SRM, reducing the search space and contributing to the design of more efficient machines.

Jones and Nachtsheim [16] proposed a new class of three-level designs that provide estimates of main effects that are not biased by any second-order effect, require only one more than twice as many runs as there are factors, and avoid confounding of any pair of second-order effects. The number of experiments required is very low compared to other methods, even if all the SRM design variables are considered, and this is a decisive factor in the choice of this DSD class. For  $m$  factors only  $2m + 1$  experiments are required, which is much lower than the amount of experiments required for other classes, such as  $3^m$  by factorial experiment and  $2^m + 2m + 1$  required by central composite design. Thus, the computational cost of the following analysis can be greatly reduced.

The SRM studied is a four-phase motor with eight stator poles and six rotor poles. The effects on the variables  $D_i$ ,  $D_o$ ,  $L$ ,  $g$ ,  $\beta_s$ ,  $\beta_r$ ,  $b_{sy}$ , and  $b_{ry}$  will be analyzed, thus totaling 17 experiments performed. The responses chosen to analyze SRM performance are average torque and machine losses. The experiments performed are finite element simulation performed in FEMM software. The parameters of the SRM studied are shown in **Table 2**, which also presents machine details and the range adopted for each design variable according to the design guidelines shown in Section 3.

To perform these experiments, three software will be used. Minitab is a statistical software that will help design the experiment and get the results. MATLAB is used to perform the calculations and obtain the results of finite element simulations computed through FEMM.

#### 4.1 Effects on average torque

The effects of changes in dimension values can be determined in several ways; in this work the statistical results obtained through Minitab will be presented. The Pareto graph is an important quality tool and allows visualization of the effects

ranked by the magnitude of their contribution [35]. **Figure 8** shows the Pareto chart of the standardized effects for the average torque. The Pareto chart shows the absolute values of the standardized effects from the greatest effect to the smallest effect. The standardized effects are t-statistics that test the null hypothesis that the effect is zero. The greater the magnitude of the standardized effect, the greater the evidence against the null hypothesis, that is, the greater the probability that there is a significant difference.

From **Figure 8** we can determine which factors cause a greater impact on the average torque value; however, it is not possible to know how each dimension affects the response. The normal plot of standardized effects, shown in **Figure 9**, shows which effects are positive and negative. Positive effects, right of the line, increase the response when the factor changes from low to high value. Negative effects, left of the line, decrease the response when factor definitions change from low to high. Effects further from 0 are more statistically significant.

Through the results presented in **Figures 8 and 9**, it is possible to draw important conclusions about the influence of dimensions on the average torque value. The three dimensions that most influence the average torque value are the rotor polar

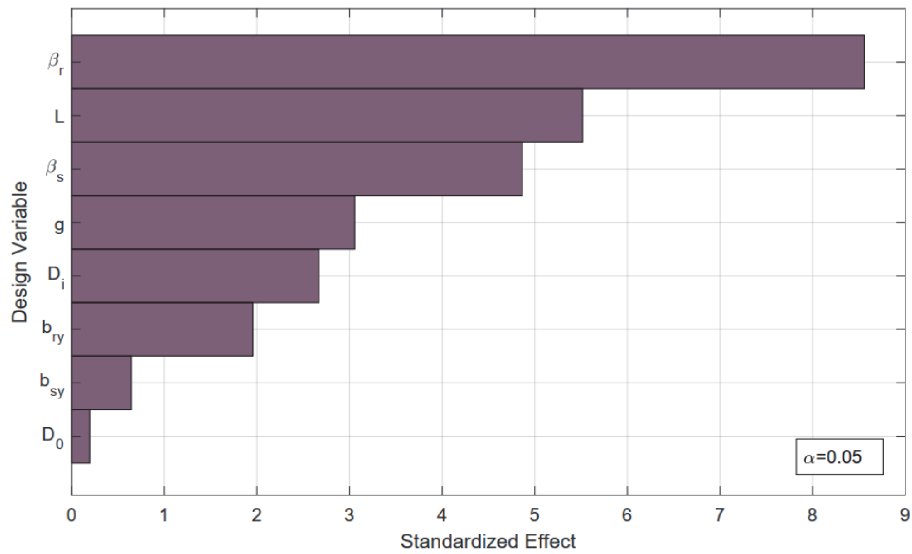


**Figure 8.**  
Pareto chart of the standardized effects for average torque ( $T_{ave}$ ).

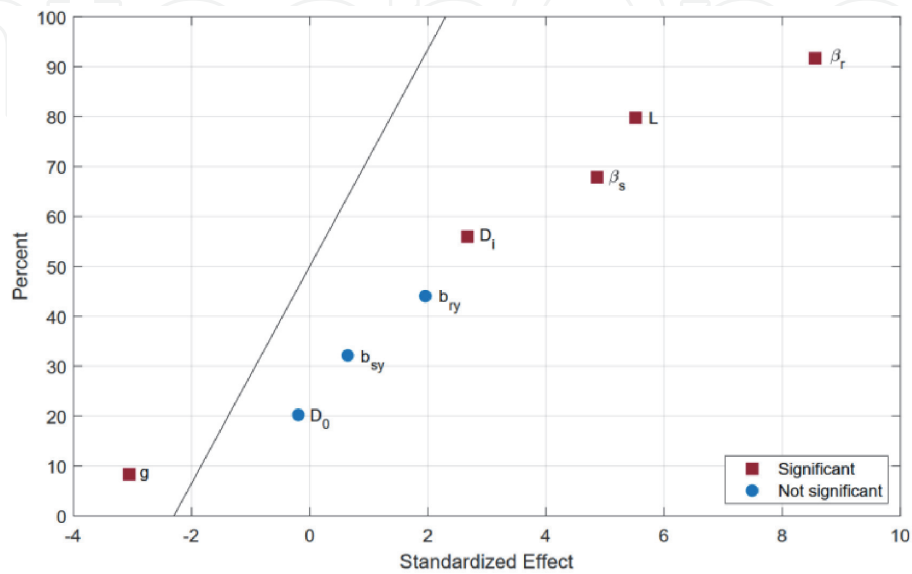


**Figure 9.**  
Normal plot of the standardized effects for average torque ( $T_{ave}$ ).

arc ( $\beta_r$ ), the core length ( $L$ ), and the stator polar arc ( $\beta_s$ ). The polar arcs determine the energy conduction angle and thus the torque production interval and the average torque value (see **Figure 2**). In turn, the core length is a fundamental parameter and directly proportional to the torque value because it allows more energy to be converted into the machine. However, increasing the value of  $L$  corresponds to increasing the material volume and cost of the machine.

Of less importance, but still significant, the air gap length and inner diameter also play important roles. Of the five significant factors presented in **Figure 9**, only the air gap has a negative effect on the average torque value, i.e., as the air gap increase, the torque value decreases. The stator and rotor polar arcs, core length, and inner diameter have a positive effect.

#### 4.2 Effects on total losses

When designing a machine, the designer should not be concerned only with the developed power and torque; the amount of losses and efficiency is often a decisive factor for the choice of the machine. Therefore, it is important to know how each dimension influences the value of the total losses, which is the sum of the losses in the windings and in the core. Losses were calculated as presented in Section 3, and in [33], mechanical losses are not considered. **Figure 10** shows the Pareto chart of standardized effects for losses, and **Figure 11** shows the normal plot of standardized effects.

According to the graphs presented, the stator polar arc and core length are the two dimensions that have the greatest impact on the losses value. This is because higher stator polar arc values cause increased losses in both copper and core as it increases the mean length of the winding, iron volume, and SRM saturation. The factor that causes the second major impact is core length as it has the greatest influence on copper losses, since the longer the core length, the longer the mean length of the winding.

The other dimensions have minor impact on the value of the losses, mainly because they cause change in only one part of the losses, copper losses, or core losses, so the total effect is smaller. Thus, the dimensions that affect the winding are more significant because copper losses represent the vast majority of losses of an electric machine.

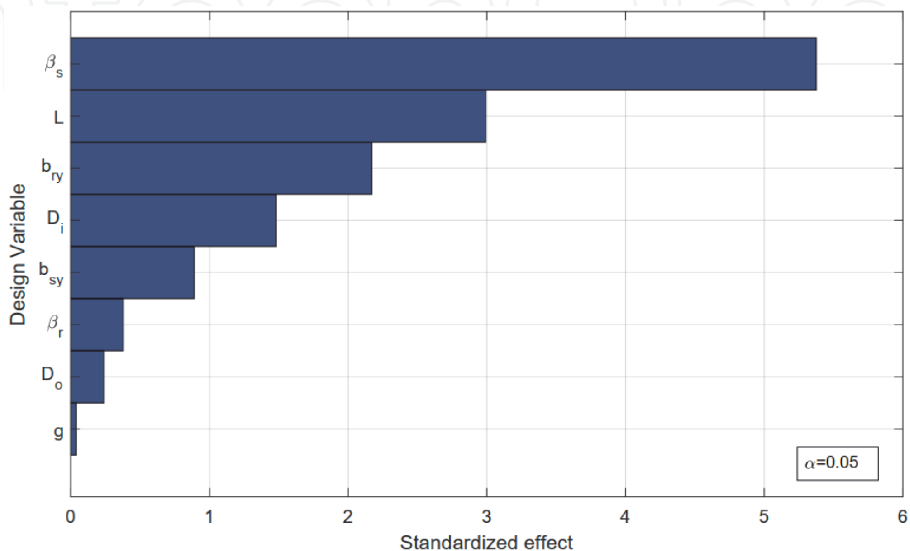


**Figure 10.**  
Pareto chart of the standardized effects for total losses ( $P_H$ ).



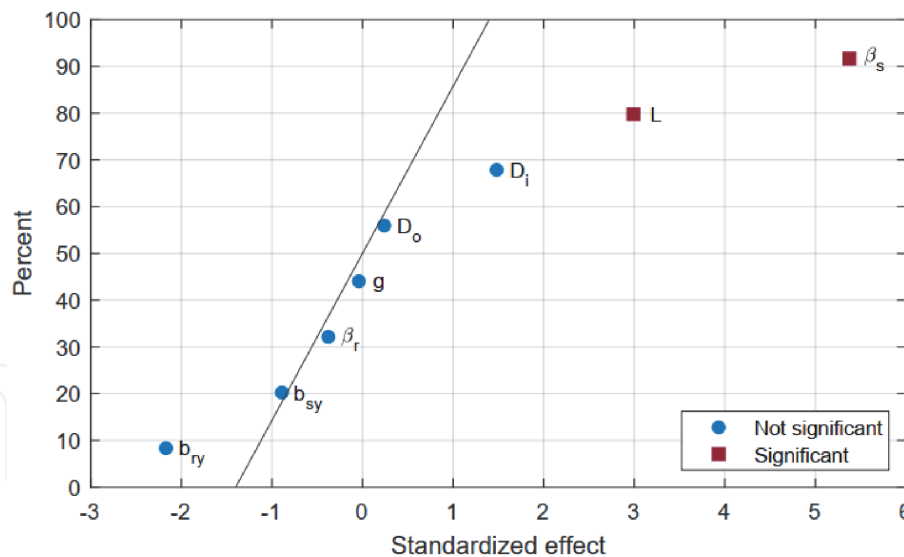


**Figure 11.**  
Normal plot of the standardized effects for total losses ( $P_{tl}$ ).

## 5. Conclusions

This chapter focused on detailed explanation of the design procedures of switched reluctance machines, for which the contributions of several authors are summarized and presented to the reader. At the outset, the structure and operation of SRM are presented. Subsequently, the SRM design procedures are presented, and we can observe that the authors sometimes disagree on the values and procedures.

Many dimensions are chosen through intervals, and this choice is often made subjectively and empirically. This fact justified the second part of this chapter, which is an analysis of the effects of dimensions on SRM performance. For this purpose, we used definitive screening design, a class of design of experiments that allows analysis of the effects of each factor with a reduced number of simulations. The impact of eight dimensions on the average torque value and on SRM losses was analyzed, the experiments were conducted through finite element simulations, and the analysis was performed by statistical software.

For the average torque, the most important dimensions are the polar arcs and the core length, since the relationship between the polar arcs determines the torque production interval and, therefore, the average torque value. However, the stator pole arc and core length are the two most significant factors for losses, and this can compromise the machine's efficiency. These results show that changes in dimensions must be made carefully and that effect analysis is important to draw these conclusions.

The results presented by the effect analysis complement the design procedures and become a useful tool for beginner designers. This data provides an insight into how each variable affects machine performance, which is important information on which choices are based at the design stage.

## Acknowledgements

The authors thank CAPES (Coordination for the Improvement of Higher Level Personnel Agency) of the Brazilian Ministry of Education for the resources allocated to the development of this research work.

IntechOpen

### Author details


Ana Camila Ferreira Mamede<sup>1\*</sup>, José Roberto Camacho<sup>1</sup> and Rui Esteves Araújo<sup>2</sup>

<sup>1</sup> Federal University of Uberlandia, Uberlandia, Minas Gerais, Brazil

<sup>2</sup> INESC TEC and Faculty of Engineering of the University of Porto, Porto, Portugal

\*Address all correspondence to: [anacamilamamede@gmail.com](mailto:anacamilamamede@gmail.com)

### IntechOpen

© 2020 The Author(s). Licensee IntechOpen. Distributed under the terms of the Creative Commons Attribution - NonCommercial 4.0 License (<https://creativecommons.org/licenses/by-nc/4.0/>), which permits use, distribution and reproduction for non-commercial purposes, provided the original is properly cited. 

## References

- [1] Lawrenson P, Stephenson J, Fulton N, Blenkinsop P, Corda J. Variable-speed switched reluctance motors. *IEE Proceedings B Electric Power Applications*. 1980;**127**(4): 253-265
- [2] Pyrhönen J, Jokinen T, Hrabovcová V. *Design of Rotating Electrical Machines*. 2nd ed. Chichester: John Wiley & Sons; 2014
- [3] Somesan L, Padurariu E, Viorel I. Two simple analytical models, direct and inverse, for switched reluctance motors. *Progress in Electromagnetics Research*. 2013;**29**:279-291
- [4] Besmi M. Geometry design of switched reluctance motor to reduce the torque ripple by finite element method and sensitive analysis. *Journal of Electric Power and Energy Conversion Systems*. 2016;**1**(1):23-31
- [5] Teixeira V, Oliveira D, Pontes R, Viana S. Influence of the switched reluctance machines design parameters on its steady-state operation characteristics. In: 2007 International Conference on Electrical Machines and Systems (ICEMS). Seoul; 2007. pp. 1455-1459
- [6] Krishnan R. *Switched Reluctance Motor Drives: Modeling, Simulation, Analysis, Design, and Applications*. Boca Raton, Florida: CRC Press; 2001
- [7] Balaji M, Kamaraj V. Evolutionary computation based multi-objective pole shape optimization of switched reluctance machine. *International Journal of Electrical Power & Energy Systems*. 2012;**43**(1):63-69
- [8] Duraković B. Design of experiments application, concepts, examples: State of the art. *Periodicals of Engineering and Natural Sciences*. 2017;**5**(3):421-439
- [9] Duraković B, Bašić H. Textile cutting process optimization model based on six sigma methodology in a medium-sized company. *Journal of Trends in the Development of Machinery and Associated Technology*. 2012;**16**(1): 107-110
- [10] Paulo F, Santos L. Design of experiments for microencapsulation applications: A review. *Materials Science and Engineering: C*. 2017;**77**: 1327-1340
- [11] Yu P, Low M, Zhou W. Design of experiments and regression modelling in food flavour and sensory analysis: A review. *Trends in Food Science and Technology*. 2018;**71**:202-215
- [12] Schlueter A, Geyer P. Linking BIM and design of experiments to balance architectural and technical design factors for energy performance. *Automation in Construction*. 2018;**86**: 33-43
- [13] Hibbert D. Experimental design in chromatography: A tutorial review. *Journal of Chromatography B*. 2012;**910**: 2-13
- [14] Garud S, Karimi I, Kraft M. Design of computer experiments: A review. *Computers and Chemical Engineering*. 2017;**106**:71-95
- [15] Ma C, Qu L. Multiobjective optimization of switched reluctance motors based on design of experiments and particle swarm optimization. *IEEE Transactions on Energy Conversion*. 2015;**30**(3):1144-1153
- [16] Jones B, Nachtsheim C. A class of three-level designs for definitive screening in the presence of second-order effects. *Journal of Quality Technology*. 2011;**43**(1):1-15

- [17] Tang Y. Characterization, numerical analysis, and design of switched reluctance motors. *IEEE Transactions on Industry Applications*. 1997;**33**(6): 1544-1552
- [18] Raminosoa T, Blunier B, Fodorean D, Miraoui A. Design and optimization of a switched reluctance motor driving a compressor for a PEM fuel-cell system for automotive applications. *IEEE Transactions on Industrial Electronics*. 2010;**57**(9): 2988-2997
- [19] Miller T. *Switched Reluctance Motors and Their Control*. Oxford: Magna Physics; 1993
- [20] Shoujun S, Weiguo L, Peitsch D, Schaefer U. Detailed design of a high speed switched reluctance starter/generator for more/all electric aircraft. *Chinese Journal of Aeronautics*. 2010; **23**(2):216-226
- [21] Elhomdy E, Li G, Liu J, Bukhari S, Cao W. Design and experimental verification of a 72/48 switched reluctance motor for low-speed direct-drive mining applications. *Energies*. 2018;**11**(1):192
- [22] Rafajdus P, Peniak A, Peter D, Makys P, Szabo L. Optimization of switched reluctance motor design procedure for electrical vehicles. In: 2014 International Conference on Optimization of Electrical and Electronic Equipment (OPTIM). Bran, Romania; 2014. pp. 397-404
- [23] Wang Y. Switched reluctance motor analysis and design for a lunar roving vehicle [Master thesis]. Montreal, Canada: McGill University; 2013
- [24] Vijayraghavan P. Design of switched reluctance motors and development of a universal controller for switched reluctance and permanent magnet brushless DC motor drives [PhD thesis]. Blacksburg, USA: Virginia Polytechnic Institute and State University; 2001
- [25] International Electrotechnical Commission. IEC 60072-1:1991. Dimensions and output series for rotating electrical machines - Part 1: Frame numbers 56 to 400 and flange numbers 55 to 1080. 6th ed. 1991
- [26] Riba J, Garcia A, Romero I. An educational tool to assist the design process of switched reluctance machines. *International Journal of Electrical Engineering Education*. 2016; **54**(1):35-56
- [27] Naayagi R, Kamaraj V. Optimum pole arcs for switched reluctance machine with reduced ripple. In: 2005 International Conference on Power Electronics and Drives Systems. Kuala Lumpur, Malaysia; 2005. pp. 761-764
- [28] Xue X, Cheng K, Ng T, Cheung N. Multi-objective optimization design of in-wheel switched reluctance motors in electric vehicles. *IEEE Transactions on Industrial Electronics*. 2010;**57**(9): 2980-2987
- [29] Sheth N, Rajagopal K. Optimum pole arcs for a switched reluctance motor for higher torque with reduced ripple. In: 2003 IEEE International Magnetism Conference (INTERMAG). Boston, USA. 2003. p. CP-06
- [30] Radun A. Design considerations for the switched reluctance motor. *IEEE Transactions on Industry Applications*. 1995;**31**(5):1079-1087
- [31] Radun A. Analytically computing the flux linked by a switched reluctance motor phase when the stator and rotor poles overlap. *IEEE Transactions on Magnetism*. 2000;**36**(4):1996-2003
- [32] Sheth N, Rajagopal K. Estimation of core loss in a switched reluctance motor

based on actual flux variations. In: 2006 International Conference on Power Electronic, Drives and Energy Systems. New Delhi, India: 2006. pp. 1-5

[33] Materu P, Krishnan R. Estimation of switched reluctance motor losses. IEEE Transactions on Industry Applications. 1992;**28**(3):668-679

[34] Hayashi Y, Miller T. A new approach to calculating core losses in the SRM. IEEE Transactions on Industry Applications. 1995;**31**(5):1039-1046

[35] Juran J, Godfrey A. Juran's Quality Handbook. 5th ed. New York, USA: McGraw-Hill Professional Publishing; 1998